Geosci. Model Dev. Discuss., https://doi.org/10.5194/gmd-2018-33
Manuscript under review for journal Geosci. Model Dev.
Discussion started: 19 March 2018

Geoscientific Model Development Discussions

Physical parametrisation of fire-spotting for operational fire spread models: response analysis with a model based on the Level Set Method

Inderpreet Kaur[1], Anton Butenko[2,3], and Gianni Pagnini[4,5]

[1]Department of Atmospheric Chemistry, Max Planck Institute for Chemistry, Mainz, Germany
[2]Space Research Institute of Russian Academy of Sciences, Moscow, Russia
[3]Institute of Geography, University of Bremen, Bremen, Germany
[4]BCAM–Basque Center for Applied Mathematics, Bilbao, Basque Country – Spain
[5]Ikerbasque–Basque Foundation for Science, Bilbao, Basque Country – Spain

Correspondence: Gianni Pagnini (gpagnini@bcamath.org)

Abstract. Fire-spotting is often responsible for a dangerous flare up in the wildfire and causes secondary ignitions isolated from the primary fire zone leading to perilous situations. In this paper a complete physical parametrisation of fire-spotting is presented within a formulation aimed to include random processes into operational fire spread models. This formulation can be implemented into existing operational models as a post-processing scheme at each time step, without calling for any major changes in the original framework. In particular, the efficacy of this formulation has already been shown for wildfire simulators based on an Eulerian moving interface method, namely the Level Set Method (LSM) that forms the baseline of the operational software WRF-SFIRE, and for wildfire simulators based on a Lagrangian front tracking technique, namely the Discrete Event System Specification (DEVS) that forms the baseline of the operational software FOREFIRE. The simple and computationally less expensive parametrisation includes the important parameters necessary for describing the landing behavior of the firebrands. The results from different simulations with a simple model based on the LSM highlight the response of the parametrisation to varying fire intensities, wind conditions and different firebrand radii. The contribution of the firebrands towards increasing the fire perimeter varies according to different concurrent conditions and the simulation results prove to be in agreement with the physical processes. Among the many rigorous approaches available in literature to model the firebrand transport and distribution, the approach presented here proves to be simple yet versatile for application to operational fire spread models.

1 Introduction

Fire-spotting is an important phenomenon associated with the wildfires (Fernandez-Pello, 2017). It is documented as a dominant phenomenon contributing towards a rampant spread of fire in many devastating historical fires (Koo et al., 2010). Spot

Geosci. Model Dev. Discuss., https://doi.org/10.5194/gmd-2018-33
Manuscript under review for journal Geosci. Model Dev.
Discussion started: 19 March 2018

Geoscientific Model Development Discussions

fires occur when fragments of the fuel tear off from the main fuel source and the horizontal wind transports the burning embers beyond the zone of direct ignition. The burning embers/firebrands can develop new secondary ignition spots and lead to a perilous increase in the effective rate of spread (ROS) of the fire. Researchers have tried to understand the phenomenology of fire-spotting through both experimental and theoretical aspects to update the existing wildfire management decision support systems. Most of the experimental procedures for studying the fire-spotting phenomenon focus on characterization of the generation of firebrands (Manzello et al., 2007; El Houssami et al., 2016; Thomas et al., 2017), shape and size of the firebrands (Manzello et al., 2009; Tohidi et al., 2015), drag forces and ignition processes (Manzello et al., 2008). The short temporal and spatial scales of the experiments limit a detailed description of the landing distributions and the flight paths of the firebrands. On the other hand, the firebrand transport models provide an estimate of the maximum landing distance and flight paths of the firebrands through a simplified overview of the physical dynamics of the fire behavior, plume characteristics, and the atmospheric conditions around the fire. Tarifa et al. (1965, 1967) and Albini (1979, 1983) were the foremost to develop simplified plume models for an estimation of firebrand lifetimes, flight paths and the potential fire-spotting distance. Beginning with their works, there has been a paradigm shift in the development of the firebrand transport models, with the latest models benefiting from the advanced computational techniques and resources.

Woycheese et al. (1999) provide a model for the lofting of spherical and cylindrical firebrands by using the plume model proposed by Baum and McCaffrey (1989). They suggest analytical functions for the maximum loftable diameter and the maximum loftable height in terms of the fire intensity, atmospheric wind and the fuel characteristics. Numerical experiments by Sardoy and co-workers (Sardoy et al., 2007, 2008) also analyze the effect of atmospheric conditions, fire properties and fuel properties on the firebrand behavior and provide a statistical estimate of the ground level distributions of the disk shaped firebrands. Their results highlight that firebrands landing at short distances (up to $1000\,\mathrm{m}$ from the source) follow a lognormal distribution. A study by Wang (2011) also provides a mathematical model to quantify the distribution and the mass of the firebrands through a Rayleigh distribution function. In an another study, Koo et al. (2007) present a physics based multiphase transport model for wildfires (FIRETEC) to study the firebrand transport. In a recent study, Martin and Hillen (2016) also discuss the underlying physical processes for firebrands in detail and they derive a landing distribution based on these physical processes. Besides these statistical approaches, few numerical models based on Large Eddy Simulation (LES) (Himoto and Tanaka, 2005; Thurston et al., 2017; Tohidi and Kaye, 2017) or Computational Fluid Dynamics (CFD) (Wadhwani et al., 2017), small world networks (Porterie et al., 2007), cellular automata models (Perryman et al., 2013) also exist in the literature. Bhutia et al. (2010) present one such study based on coupled fire/atmosphere LES for predicting the short range fire-spotting. They simulate multiple firebrand trajectories for analyzing the sensitivity of the flight path to different particle sizes, release heights and wind conditions but also mention the limited applicability of such models to operational use due to the computational demands.

Despite the presence of multiple studies focusing on the detailed aspects of the firebrand landing distributions, none of the them is able to provide a comprehensive yet versatile approach for an application to operational fire spread models. The continuing demand for the operational management tools is to provide a quick and efficient output with simple inputs but at the same time taking the most important parameters into consideration. Few operational fire spread models like FARSITE (Finney,

Geosci. Model Dev. Discuss., https://doi.org/10.5194/gmd-2018-33
Manuscript under review for journal Geosci. Model Dev.
Discussion started: 19 March 2018

1998), BEHAVEPLUS (Andrews and Chase, 1989) and Prometheus (Tymstra et al., 2010) incorporate the phenomenon of fire-spotting through the Albini's model (Albini, 1979, 1983). But Albini's model provides only an estimate of the maximum distance for a spot fire and does not include any function for the ignition probability to model the spread of spot fires. The Australian wildfire simulator PHOENIX Rapidfire (Tolhurst et al., 2008) is designed to model large fast moving fires and also includes a fire-spotting module, but the formulations for fire spread in PHOENIX are calibrated for eucalyptus forests and a generic application to other types of fuels requires a re-calibration (Pugnet et al., 2013). The new operational models like WRF-SFIRE (Mandel et al., 2011) and FOREFIRE (Filippi et al., 2009) are fast and allow coupling with the atmospheric models for a better representation of the initial and concurrent atmospheric conditions; but lack any specific module to tackle the fire-spotting behavior.

In this article, the authors complete the statistical formulation proposed by Pagnini and Mentrelli (2014) to model the fire-brand landing distribution by introducing a physical parametrisation of the fire-spotting phenomenon. The physical parametrisation of the probabilistic model is developed to incorporate the fire-spotting behavior in terms of the fire intensity, wind conditions and fuel characteristics. This formulation is independent of the method used for the fire-line propagation and the definition of the ROS, and is versatile enough to be utilized with any of the existing operational fire spread models. In their previous work (Kaur et al., 2016), the authors demonstrate the applicability of the formulation to two wildfire models based on different fire-line propagation methods, i.e. a Eulerian moving interface method based on the Level Set Method (LSM) that is the basis for the WRF-SFIRE model and a Lagrangian front tracking technique based on the Discrete Event System Specification (DEVS) that is the basis for the FOREFIRE model. The aim of the present study is to provide a simple yet complete addition to operational fire spread models for representing the random behavior of fire-spotting through simple inputs related to the wildfires. This probabilistic model is devised to provide a physical meaning to the spread of fire by virtue of firebrands. Results from different simulations are presented to highlight the sensitivity of the simple parametrisation in simulating the behavior of firebrands under different wind conditions and fire intensities. The formulation to include random process and the proposed physical parametrisation are implemented into a simple fire spread model based on the LSM.

The remaining part of the article is organized as follows. Section 2 presents a very brief description of the mathematical model, while the physical parametrisation of fire-spotting within the framework of a lognormal distribution of the landing distance is described in section 3. Section 4 describes the set-up of the numerical simulations. Section 5 describes the results pertaining to different numerical simulations and the conclusions are drawn in section 6.

2 Model formulation

A mathematical model to represent the random effects associated with the wildland fires has been developed by Pagnini and co-authors (Pagnini and Massidda, 2012b, a; Pagnini, 2013, 2014; Pagnini and Mentrelli, 2016, 2014; Kaur et al., 2015, 2016; Mentrelli and Pagnini, 2016). This formulation describes the motion of the fire-line as a composition of the drifting part and the fluctuating part. The drifting part represents the fire-perimeter obtained through the definition of the ROS based on fuel characteristics and the averaged fire properties. The output from most of the existing operational fire spread models can be

Geosci. Model Dev. Discuss., https://doi.org/10.5194/gmd-2018-33
Manuscript under review for journal Geosci. Model Dev.
Discussion started: 19 March 2018

Geoscientific Model Development Discussions

considered as the drifting part. On the other hand, the fluctuating part is independent of the drifting part and represents the additional contribution to the fire-perimeter as an effect of the random processes like turbulence and fire-spotting. This model can be implemented as a crucial addition to operational fire spread models through a post processing application at each time step. The drifting component obtained from the output of any wildfire model can be updated with the fluctuating component at each time step to include the effects of turbulence and fire-spotting. A brief overview of the mathematical details has been provided in this section; for a detailed description the interested readers are referred to (Pagnini and Mentrelli, 2014; Kaur et al., 2016).

In a domain S, let $\Omega \subseteq S$ represent the burnt area and let $X^\omega = X + \eta^\omega$ represent the trajectory of each active fire point as the sum of a drifting part X and a fluctuating part η^ω. The drifting part X is obtained from the output of a wildfire propagation model, while the fluctuations in the fire-line are included through a probability density function (PDF) corresponding to the type of random process under consideration. Let the area enclosed by the drifting part be described through an indicator function $I_\Omega(\boldsymbol{x},t) = 1$ when $\boldsymbol{x}$ is inside the domain Ω, and $I_\Omega(\boldsymbol{x},t) = 0$ when $\boldsymbol{x}$ is outside. Considering the ensemble average of the active burning points, a new effective indicator function is defined as:

$$\phi_e(\boldsymbol{x},t) = \int_S I_\Omega(\overline{\boldsymbol{x}},t) f(\boldsymbol{x};t|\overline{\boldsymbol{x}}) d\overline{\boldsymbol{x}}\,, \tag{1}$$

where, $f(\boldsymbol{x};t|\overline{\boldsymbol{x}})$ represents the PDF which accounts for the fluctuations of the random effects. The effective indicator $\phi_e \in [0,1]$ and an arbitrary threshold is fixed to mark points as burned, i.e., $\Omega(\boldsymbol{x},t) = \{\boldsymbol{x} \in S \mid \phi_e(\boldsymbol{x},t) > \phi_e^{th}\}$. The ignition of the fuel by the firebrands involves heat exchange over a sufficient period of time, hence, a sufficient delay is also incorporated in the model through an other function ψ. The function ψ simulates the ignition of fuel by hot air and burning embers as an accumulative process over time:

$$\psi(\boldsymbol{x},t) = \int_0^t \phi_e(\boldsymbol{x},\eta) \frac{d\eta}{\tau}\,, \tag{2}$$

where τ is the ignition delay. All points with $\psi(\boldsymbol{x},t) > 1$ are labeled as burned when $\phi_e(\boldsymbol{x},t) > \phi_e^{th}$.

The shape of the PDF is established by analyzing the random processes under consideration. The diversity in the shapes of the PDF provides the model a multifaceted outlook. Assuming fire-spotting to be a downwind phenomenon occurring in turbulent atmosphere the shape of the PDF is defined as follows:

$$f(\boldsymbol{x};t|\overline{\boldsymbol{x}}) = \begin{cases} \displaystyle\int_0^\infty G(\boldsymbol{x} - \overline{\boldsymbol{x}} - l\,\hat{\boldsymbol{n}}_U;t) q(l)\, dl\,, & \text{downwind}\,, \\ \\ G(\boldsymbol{x} - \overline{\boldsymbol{x}};t)\,, & \text{upwind}\,. \end{cases} \tag{3}$$

The distribution function $G(\boldsymbol{x} - \overline{\boldsymbol{x}};t)$ is an isotropic bi-variate Gaussian and provides for the effect of the turbulent heat fluxes in fire propagation while, the distribution function $q(l)$ represents the firebrand landing distribution. The strength of the turbulence

Geosci. Model Dev. Discuss., https://doi.org/10.5194/gmd-2018-33
Manuscript under review for journal Geosci. Model Dev.
Discussion started: 19 March 2018

Geoscientific Model Development Discussions

around the fire is parametrised through a turbulent diffusion coefficient $\mathscr{D}$. A short description of the physical characterisation of $\mathscr{D}$ is presented in the next section. A precise description of the landing distributions through experimental observations is difficult due to temporal and spatial constraints. But the experimental results analysing the flight paths, shape and landing distributions of the firebrands have shown that the frequency of the firebrands landing in the positive direction from the source increases with distance to a maximum value and then gradually decays to zero (Hage, 1961). The landing distributions of the firebrands have also been studied though the numerical solution of the energy balance equations (Sardoy et al., 2008; Himoto and Tanaka, 2005; Kortas et al., 2009). Among the different transport models proposed in literature, both Sardoy et al. (2008) and Himoto and Tanaka (2005) describe the lognormal density function as an approximate fit to the landing distribution of the firebrands. Whereas, Wang (2011) proposes a Rayleigh distribution for the same. In this article, the shape of $q(l)$ is defined by a lognormal distribution to describe the frequency profile of the fallen firebrands:

$$q(l) = \frac{1}{\sqrt{2\pi}\sigma l} \exp \frac{-(\ln l/\mu)^2}{2\sigma^2}, \tag{4}$$

where μ is the ratio between the square of the mean of landing distance l and its standard deviation, while σ is the standard deviation of $\ln l/\mu$.

3 Physical parametrisation of fire-spotting

The firebrands generated from the vegetation face strong buoyant forces and the ones with size less than the maximum loftable size are uplifted vertically in the convective column. These firebrands rise to a maximum height till the buoyant and the gravitational forces counterbalance each other. Once the firebrands are expelled from the column, they are steered by the atmospheric wind and they fly at their terminal velocity of fall. The simplified models for the landing distance assume that the ejection of the firebrands from the vertical convective column is a random process affected by the turbulence in the environment around the fire. Among other factors, the strength of the convective column, the atmospheric conditions and the dimensions of the firebrands play a vital role in governing the trajectory of the firebrands. In this section, the landing distribution of the firebrands based on a lognormal probability function is combined with the physical characterization of the firebrand transport. The parametrisation presented here is simplified and includes only the vital ingredients necessary to describe the firebrand transport. Each firebrand is assumed to be spherical and for a particular set of concurrent atmospheric conditions and fuel characteristics the size is assumed to be constant. Any modification in the flight of the firebrand due to changing wind fields, rotation of firebrand or collision with other firebrands is also neglected. Prelimary results were discussed in Kaur and Pagnini (2016).

Assuming the shape of the firebrands to be spherical, Tarifa et al. (1965) combines both experimental and theoretical approaches to characterise the maximum landing distances of the firebrands. Based on these results, Wang (2011) provides an approximation of the maximum travel distance for spherical firebrands from a vertical convective column in terms of the maximum loftable height $\mathcal{H}$, the mean wind U and the radius of the firebrands r:

$$\mathcal{L} = \mathcal{H}\left(\frac{3U^2\rho_a C_d}{2\rho_f r g}\right)^{1/2}, \tag{5}$$

Geosci. Model Dev. Discuss., https://doi.org/10.5194/gmd-2018-33
Manuscript under review for journal Geosci. Model Dev.
Discussion started: 19 March 2018

Geoscientific Model Development Discussions

where ρ_a and ρ_f represent the density of the ambient air and of the wildland fuels respectively, C_d is the drag coefficient and g is the acceleration due to gravity. The maximum height reached by the convective column limits the maximum height which any of the lofted firebrands can attain. Hence, the vertical dimension of the column is assumed to be an estimate of the maximum loftable height $\mathcal{H}$. The height of the convective column can be derived from both remote sensing data and analytical formulations. Fire plume injection heights derived by Multi-angle Imaging Spectro Radiometer (MISR) serve as a surrogate for the plume height measurements (MISR Plume Height Project, https://misr.jpl.nasa.gov/getData/accessData/MisrMinxPlumes2/). In addition to the remote sensing observations, analytical formulations defining the plume height in terms of the fire intensity are also present in literature. Sofiev et al. (2012) state one of such formula for the plume height in terms of the fire radiative power (FRP) and Brunt Väisälä frequency N. FRP is the radiative fire intensity I for a unit depth of the combustion zone d and is often used as a proxy for fire intensity. Adapting the formula by Sofiev et al. (2012) in terms of fire intensity gives:

$$\mathcal{H} = \alpha H_{abl} + \beta \left(\frac{I}{d P_{f0}} \right)^{\gamma} \exp\left(\frac{\delta N_{FT}^2}{N_0^2} \right), \tag{6}$$

where $\alpha = 0.24$, $\beta = 170\,\mathrm{m}$, $\gamma = 0.35$ and $\delta = 0.6$ are empirical constants, $P_{f0} = 10^6\,\mathrm{W}$ is the reference fire power, H_{abl} is the height of the atmospheric boundary layer and subscript FT refers to the free troposphere.

Assuming the maximum landing distance to be represented by the p^{th} percentile of the lognormal distribution, the landing distance can be written as:

$$\mathcal{L} = \mu \exp(z_p \sigma), \tag{7}$$

where the value of z_p corresponding to the p^{th} percentile can be estimated from the z-tables (`http://www.itl.nist.gov/div898/`). To ascertain the value of the cut-off percentile, it is assumed that the effective contribution of the firebrands cease to be meaningful when their probability falls by 20 times its peak value. Thereafter, the ability of the firebrands to cause an ignition is assumed to be negligible. For a lognormal distributions with shape parameters comparable to the simulation test cases shown here, the probability distribution tends to have an extremely sharp rise and a gradual decay. For this particular distribution, the cutoff for 50th percentile lies way beyond the point denoting the 1/20th of the maximum probability. In order to define a generalized value of the cutoff percentile for all the simulation cases presented in this article, the value of z_p is chosen to be 0.45, which corresponds to the 67^{th} percentile point. Further, using Eq. (5) and Eq. (7), the lognormal shape parameters μ and σ can be physically parametrised as follows:

$$\mu = \mathcal{H} \left(\frac{3 \rho_a C_d}{2 \rho_f} \right)^{1/2}, \tag{8}$$

$$\sigma = \frac{1}{2 z_p} \ln\left(\frac{U^2}{r g} \right). \tag{9}$$

In this parametrisation of the fire-spotting, the quantification of μ and σ is chosen to provide a most rational description for the transport of firebrands. The parameter μ is parametrised to characterize the lofting of the firebrands inside the convective

Geosci. Model Dev. Discuss., https://doi.org/10.5194/gmd-2018-33
Manuscript under review for journal Geosci. Model Dev.
Discussion started: 19 March 2018

Geoscientific Model Development Discussions

column. The relative density and atmospheric drag quantify the buoyant forces experienced by the firebrand; hence it is appropriate to include these quantities in the definition of μ to describe the maximum allowable height for each firebrand in varying fire intensities. The density ratio ρ_a/ρ_f also limits the maximum allowable height for each firebrand. On the other hand, σ is parametrised to define the transport of the firebrands under the effect of the wind after they are ejected from the convective column. In a wind driven regime of fire-spotting, the flight path of the firebrand is affected by its size and firebrands beyond a critical size cannot be steered by the prevailing wind. This critical size is defined as the maximum liftable radius $r_{max} = U^2/g$. It is interesting to note that the dimensionless ratio $U^2/(rg)$ is also known as the Froude number and quantifies the balance between the inertial and the gravitational forces experienced by the firebrand.

In this model, the phenomenon of fire-spotting is assumed to occur together with the turbulent heat flux around the fire, and the turbulent diffusion coefficient $\mathscr{D}$ is utilised as a measure of the turbulent heat transfer generated by the fire. It is parametrised in terms of the Nusselt number Nu. Nusselt number defines the ratio between the convective and conductive heat transfer in fluids and is defined as

$$Nu = (\mathscr{D} + \chi)/\chi\,, \tag{10}$$

where χ is the thermal diffusivity of air at ambient temperature. Experimentally, it is shown that Nusselt number is related to Rayleigh number as $Nu \simeq 0.1Ra^{1/3}$ (Niemela and Sreenivasan, 2006). Rayleigh number is defined as $Ra = \gamma \Delta T g h^3/(\nu\chi)$, where γ is the thermal expansion coefficient, h is the dimension of the convective cell, ν is the kinematic viscosity and ΔT is the temperature gradient between the top and bottom faces of the convective cell.

The simple design of the physical parametrisation makes the model computationally less expensive and the requirement of defining only few vital parameters to execute any simulation also serves as an added advantage to the operational users.

4 Simulation set-up

A few idealized simulations are carried out to highlight the potential applicability of the formulation. For all the simulations, a flat domain with a homogeneous coverage of *Pinus ponderosa* ecosystem is selected. The simulations are run using a basic set-up of wildfire model which involves a moving interface method based on the LSM (Pagnini and Massidda, 2012a, b; Pagnini and Mentrelli, 2014). The Byram formula (Byram, 1959; Alexander, 1982) is used to estimate the ROS of the fire-line:

$$V(x,t) = \frac{I(1+f_w)}{H\,\alpha\,\omega_0}\,, \tag{11}$$

where I is the fire intensity, $H = 22000\,\mathrm{KJKg^{-1}}$ is the fuel low heat of combustion, $\omega_0 = 2.243\,\mathrm{Kgm^{-2}}$ is the oven-dry mass of the fuel and the functional dependence on the wind is included through the factor f_w. The user has flexibility to introduce a different ecosystem in the simulations by modifying the the parameters H and ω_0. The parameter α is chosen to guarantee that the maximum ROS is always equal to the ROS prescribed by the Byram formulation.

Sensitivity of the formulation to depict the different firebrand landing distributions is highlighted through two sets of test cases. In the first test case, the wind conditions and the size of the firebrands are assumed to be constant as the fire intensity

Geosci. Model Dev. Discuss., https://doi.org/10.5194/gmd-2018-33
Manuscript under review for journal Geosci. Model Dev.
Discussion started: 19 March 2018

Geoscientific Model Development Discussions

changes. In the second test case, the fire intensity is assumed to be non-changing and the simulations for different wind conditions are carried out. The second test case is also repeated for a different radius of the firebrand.

By assuming the size of the convective column to be 100 m and the temperature difference as 100 K, the scale of the turbulent diffusion coefficient turns out to be approximately 10^4 times the thermal diffusivity of air at ambient temperature. For all the simulations presented in this article, the value of the turbulent diffusion coefficient $\mathcal{D}$ is assumed to be $0.15\,m^2s^{-1}$. For speeding-up all simulations presented in this article, the domain has been scaled by a factor of 4 to reduce the computation time. This scaling affects the ROS and the turbulent diffusion coefficient and their value is reduced by a factor of 4. Fire intensity and the wind speed remain unaffected by the re-scaling. It is mentioned that such scaling has no effect on the outputs of the simulations but helps in reducing the computation time.

It is remarked that, in the simulations presented in this paper, the firebrands are considered to be a sphere of constant radius for each simulation; but in real situations all shapes and sizes of the firebrand are produced from the fuel. The size of the firebrand in the set-up of these test cases is assumed to be equal to the "collapse diameter". Experiments show that the firebrands with size greater than the "collapse diameter" propagate over the same distance under identical initial conditions (Woycheese et al., 1999). It is also emphasized that the selection of the domain and other parameters do not correspond to any real fire but an effort is made to chose the values of different parameters to lie in the valid range.

5 Results and Discussion

The mathematical formulation of the random effects presented in this article considers the effects of turbulence and fire-spotting together.

An aspect of the mathematical formulation for fire-spotting worth mentioning here is its ability to generate secondary fires. Top panel of Figure 1 shows the evolving fire perimeter at different time steps. The secondary fires at $60\,\mathrm{min}$ and $70\,\mathrm{min}$ mimic the action of firebrands falling away from the main fire source. As time progresses, the primary fire-line catches up with these isolated fire zones and merges them with itself. Bottom panel of Figure 1 provides a brief insight into the additional contribution due to the fire-spotting effects. The total number of burned points is plotted at different times for two simulations: only turbulence, and turbulence plus fire-spotting. All the simulation parameters remain the same in both the simulations. At lower times, fire-spotting has no visible contribution, but after $50\,\mathrm{min}$, the activity due to fire-spotting picks up and the burned area increases rapidly. At $140\,\mathrm{min}$ the increase in the burned area with the combined effect of the two random processes is three times more than turbulence alone.

Top panel of Figure 2 shows the increase in the burned area due to the combined effect of turbulence and fire-spotting when the fire intensity of the wildfire increases. Constant wind velocity ($10\,\mathrm{ms}^{-1}$) and the firebrand radius ($0.015\,\mathrm{m}$) are considered for these simulations. From the physical parametrisation of the lognormal shape parameters μ and σ, for these set of simulations (increasing the fire intensity I), the value of μ varies while σ remains constant. The effective increase in the burned area is evaluated through a parameter β_e, which describes the increase in the number of burned grid points with respect

Geosci. Model Dev. Discuss., https://doi.org/10.5194/gmd-2018-33
Manuscript under review for journal Geosci. Model Dev.
Discussion started: 19 March 2018

Geoscientific Model Development Discussions

to the simulation when no random effects are considered:

$$\beta_e = (\mathbf{x}_{random} - \mathbf{x}_{no-random})/\mathbf{x}_{no-random}\,. \tag{12}$$

According to the definition of the ROS (Eq. 11), the increase in the fire intensity causes an increase in the total burned area, but the relative change with respect to the burned area (β_e) reflects a sharp rise in the burned area followed by a gradual fall. An increase in the fire intensity shows a little variation for values between $15 - 38\,\mathrm{KWm^{-1}}$, but any further increase in I declines the effective contribution of the firebrands. In a lognormal distribution, an increase in the value of μ reduces the maximum probability, and the right tail tends to follow a very slow decay with small values of probability. In such situations, the 67^{th} percentile of the lognormal distribution represents the distance where firebrands do not have enough temperature to cause ignition. Ignition of the unburned fuel is an accumulative process, and an adequate heat transfer is required to reach the ignition temperature. According to the physical parametrisation proposed here, an increase in the fire intensity increases the plume height and causes the firebrands to be ejected from elevated heights. Higher release height contributes towards an increase in the firebrand activity at longer distances and the initial increase in the fire perimeter points follows this observation. But at the same instance, the increase in the firebrand ejection height over constant wind conditions causes the firebrands to travel longer in the atmosphere before hitting the ground. The growing travel time for a firebrand promotes its combustion and the firebrand reaches the ground with a lower temperature than its counterpart ejected at lower heights. Lower temperature of the firebrands leads to an inadequate heat exchange with the unburned fuel for a successful ignition and hence after reaching an area of maximum activity, the effective contribution of the firebrands under same atmospheric conditions diminishes with increasing plume height.

Bottom panel of Figure 2 highlights the simulation results with an increasing value of the wind velocity over constant fire intensity ($50\,\mathrm{KWm^{-1}}$). The results for two different radii ($0.015\,\mathrm{m}$ and $0.15\,\mathrm{m}$) are presented. In terms of the lognormal shape parameters, a varying U and r under constant fire intensity correspond to a varying σ and constant μ respectively. The line plot for $r = 0.015\,\mathrm{m}$ shows that the increasing wind velocity causes the effective area under fire to increase substantially. The burned area increases 50 times under the combined effect of the turbulence and fire-spotting over the case of no-random effects. After a peak firebrand contribution observed around $15\,\mathrm{ms^{-1}}$, the contribution of the firebrands decreases and at very high wind velocities (beyond $20\,\mathrm{ms^{-1}}$), the total increase in the burned area is constant. On the other hand, for the other set of simulations for radius $r = 0.15\,\mathrm{m}$, the effective increase in the area follows an identical pattern with an exception of the uniform behavior exhibited at high wind velocities. The total increase in the burned area for a larger firebrand size is also of a lesser magnitude. This response of the model over different wind velocities and firebrand radii is well contained in the nature of the lognormal distribution and the physical parametrisation of σ. Increasing the value of σ shifts the maximum of the lognormal distribution towards left with a very sharp rise. Owing to the sharp rise, the right tail follows a slow and steady decay to zero. This behavior of the lognormal is capable of replicating the effects of a strong wind over the firebrands. A strong wind can carry away the firebrands at longer distances from the main source. Historically it has been reported that strong winds coupled with extremely dry conditions formed the perfect recipe for long range fire-spotting. It is evident from Eq. (9) that an increasing value of σ can be attributed to both increasing wind velocity and decreasing fire-brand size. Strong wind speeds can loft the smaller firebrands

Geosci. Model Dev. Discuss., https://doi.org/10.5194/gmd-2018-33
Manuscript under review for journal Geosci. Model Dev.
Discussion started: 19 March 2018

to longer distances but with an increasing wind speed the combustion process quickens and the firebrands reach the ground with less temperature. This fact explains the fall in the burned area over high wind conditions. On the other hand, a larger firebrand size can sustain longer in the atmosphere but their heavier mass restricts their flight to shorter distances in comparison to the lighter firebrands. The uniform increase in the burned area for $r = 0.015\,\mathrm{m}$ mimics the situation where the activity of firebrands ceases to have any active long range contribution and turbulence plays a dominant role towards increasing the perimeter of the wildfire. Whereas, for a heavier firebrand lack of such constant behavior clearly points towards its ability to sustain longer in identical wind and fire conditions. Though not evident in the figure, the region depicting the negligible contribution from the heavier firebrands is expected to be observed beyond the range of wind speed presented in the plot.

6 Conclusions

A mathematical formulation complete with its physical parametrisation to reproduce/mimic the fire-spotting behavior is presented in this article. The simulations are performed to highlight the different responses of the model towards varying fire intensities and wind conditions. A case study with different firebrand radii is also shown. The simulations are simplified to highlight the physical applicability of the model and constant climatic conditions are assumed in the entire set-up. This parametrisation is successful in reproducing the different physical aspects of the firebrand landing behavior and provides a simple yet versatile addition to operational fire spread models.

In this model, the complexities related to the shape and density of the firebrands are not considered and for brevity they are assumed to be spherical with the diameter of the order of the "collapse diameter". The model also does not include an explicit computation of the time taken to reach the charred oxidation state, but an heating-before-burning mechanism is introduced in the mathematical formulation to serve a similar purpose. The inferences made from the simulations clearly fit within the physical aspects of the fire-spotting process. The increase in the wind speed causes an initial flare up in the fire perimeter, but in really high wind conditions, the size of the firebrand becomes an important parameter in determining their effective contribution. Firebrands of smaller sizes burn-out before they can cause ignition over landing. Similarly, with increasing fire intensities, the firebrands are ejected from higher heights have to travel longer and beyond a certain threshold they fail to have enough energy to cause ignition of the unburned fuel. Though the mathematical model presented here does not deal with these physical aspects explicitly, the simulation results from the evolution of the fire perimeter agree with the behavior of the fire-spotting process.

Though many other studies focus on the long range landing distributions of the firebrands, most of them include rigorous computational aspects like LES which limit their applicability to the operational models for wildfire propagation. The simple yet powerful probabilistic formulation presented in this paper obeys the physical aspects of the fire-spotting process and provides scope for its applicability to operational fire spread models. The simple physical parametristaion is also an added advantage for real-time application. In fact, the moving interface method utilized in this formulation to evolve the fire-line is based on LSM, which also forms the baseline of the operational model WRF-SFIRE. As a next step, the implementation of this

parametrisation into an operational model like WRF-SFIRE or FOREFIRE is planned which would also facilitate a validation with the observations to complete the study.

Code availability. The code for the fire-spotting modelling is developed in C. In the simulations presented in this article, the fire-spotting model is plugged as a post process at each time step in a LSM code. Here, a general-purpose library is utilized which aims at providing a robust and efficient tool for studying the evolution of co-dimensional fronts propagating in one-, two- and three-dimensional system. The library is written in Fortran2008/OpenMP, along with standard algorithms useful for the calculation of the front evolution by means of the classical LSM, and includes Fast Marching Method algorithms. The complete code is freely available at `https://github.com/ikaur17/firefronts`.

Competing interests. The authors declare that they have no conflict of interest.

Acknowledgements. This research is supported by the Basque Government through the BERC 2014-2017 program and by the Spanish Ministry of Economy and Competitiveness MINECO through BCAM Severo Ochoa accreditation SEV-2013-0323 and through projects MTM2013-40824-P "ASGAL", MTM2016-76016-R "MIP". The research started and mainly developed at BCAM, Bilbao, during the post-doc fellowship of IK and an intership period of AB.

Geosci. Model Dev. Discuss., https://doi.org/10.5194/gmd-2018-33
Manuscript under review for journal Geosci. Model Dev.
Discussion started: 19 March 2018

Geoscientific Model Development Discussions
Open Access
EGU

References

Albini, F. A.: Spot fire distance from burning trees: a predictive model, Technical Report INT-56, U.S. Department of Agriculture Forest Service Intermountain Forest and Range Experiment Station, 1979.

Albini, F. A.: Potential Spotting Distance from Wind-Driven Surface Fires, Research Paper INT-309, U.S. Department of Agriculture Forest Service Intermountain Forest and Range Experiment Station, 1983.

Alexander, M. E.: Calculating and interpreting forest fire intensities, Can. J. Bot., 60, 349–357, 1982.

Andrews, P. and Chase, C.: BEHAVE: Fire behavior prediction and fuel modeling system: BURN subsystem, part 2, Research Paper INT-260, USDA Forest Service, Intermountain Forest and Range Experiment Station, Ogden, Utah 84401, 1989.

Baum, H. and McCaffrey, B.: Fire induced flow field - theory and experiment, in: The Second International Symposium on Fire Safety Science', 13-17 June 1988, Tokyo, Japan, edited by Wakamatsa, T., pp. 129–148, International Association for Fire Safety Science: London, UK, 1989.

Bhutia, S., Jenkins, M. A., and Sun, R.: Comparison of Firebrand Propagation Prediction by a Plume Model and a Coupled–Fire/Atmosphere Large–Eddy Simulator, J. Adv. Model. Earth Syst., 2, Art. # 4, https://doi.org/10.3894/JAMES.2010.2.4, 2010.

Byram, G. M.: Combustion of Forest Fuels, in: Forest Fire: Control and Use, edited by Davis, K. P., pp. 61–89, McGraw Hill, New York, 1959.

El Houssami, M., Mueller, E., Thomas, J. C., Simeoni, A., Filkov, A., Skowronski, N., Gallagher, M. R., Clark, K., and Kremens, R.: Experimental procedures characterising firebrand generation in wildfires, Fire Technol., 52, 731–751, 2016.

Fernandez-Pello, A. C.: Wildland fire spot ignition by sparks and firebrands, Fire Safety J., 91, 2–10, 2017.

Filippi, J. B., Morandini, F., Balbi, J. H., and Hill, D.: Discrete event front tracking simulator of a physical fire spread model, Simulation, 86, 629–646, 2009.

Finney, M.: FARSITE: fire area simulator - model development and evaluation, Research Paper RMRS-RP-4, USDA Forest Service, Rocky Mountain Research Station, Ogden, Utah, 1998.

Hage, K. D.: On the dispersion of large particles from a 15-m source in the atmosphere, J. Appl. Meteor., 18, 534–539, 1961.

Himoto, K. and Tanaka, T.: Transport of disk-shaped firebrands in a turbulent boundary layer, in: The Eighth International Symposium on Fire Safety Science', 18–23 September 2005, Beijing, China, edited by Gottuk, D. and Lattimer, B., pp. 433–444, nternational Association for Fire Safety Science: Baltimore, MD, 2005.

Kaur, I. and Pagnini, G.: Fire-spotting modelling and parametrisation for wild-land fires, in: Proceedings of the 8th International Congress on Environmental Modelling and Software (iEMSs2016); Toulouse, France, 10–14 July (2016), edited by Sauvage, S., Sánchez-Pérez, J. M., and Rizzoli, A. E., pp. 384–391, ISBN: 978-88-9035-745-9, 2016.

Kaur, I., Mentrelli, A., Bosseur, F., Filippi, J. B., and Pagnini, G.: Wildland fire propagation modelling: A novel approach reconciling models based on moving interface methods and on reaction-diffusion equations, in: Proceedings of the International Conference on Applications of Mathematics 2015; Prague, Czech Republic, 18–21 November (2015), edited by Brandts, J., Korotov, S., Křížek, M., Segeth, K., Šístek, J., and Vejchodský, T., pp. 85–99, Institute of Mathematics – Academy of Sciences, Czech Academy of Sciences, Prague, Czech Republic, 2015.

Kaur, I., Mentrelli, A., Bosseur, F., Filippi, J.-B., and Pagnini, G.: Turbulence and fire-spotting effects into wild-land fire simulators, Commun. Nonlinear Sci. Numer. Simul., 39, 300 – 320, 2016.

Koo, E., Pagni, P., and Linn, R.: Using FIRETEC to describe firebrand behavior in wildfires., in: The Tenth International Symposium of Fire and Materials, 29–31 January 2007, San Francisco, CA., Interscience Communications: London, UK, 2007.

Koo, E., Pagni, P. J., Weise, D. R., and Woycheese, J. P.: Firebrands and spotting ignition in large-scale fires, Int. J. Wildland Fire, 19, 818–843, 2010.

Kortas, S., Mindykowski, P., Consalvi, J. L., Mhiri, H., and Porterie, B.: Experimental validation of a numerical model for the transport of firebrands, Fire Safety J., 44, 1095–1102, 2009.

Mandel, J., Beezley, J. D., and Kochanski, A. K.: Coupled atmosphere-wildland fire modeling with WRF 3.3 and SFIRE 2011, Geosci. Model. Dev., 4, 591–610, 2011.

Manzello, S. L., Maranghides, A., and Mell, W. E.: Firebrand generation from burning vegetation, Int. J. Wildland Fire, 16, 458–462, 2007.

Manzello, S. L., Shields, J. R., Cleary, T. G., Maranghides, A., Mell, W. E., Yang, J. C., Hayashi, Y., Nii, D., and Kurita, T.: On the development and characterization of a firebrand generator, Fire Safety J., 43, 258–268, 2008.

Manzello, S. L., Maranghides, A., Shields, J. R., Mell, W. E., Hayashi, Y., and Nii, D.: Mass and size distribution of firebrands generated from burning Korean pine (Pinus koraiensis) trees, Fire Mater., 33, 21–31, 2009.

Martin, J. and Hillen, T.: The Spotting Distribution of Wildfires, Appl. Sci., 6, 177–210, 2016.

Mentrelli, A. and Pagnini, G.: Modelling and simulation of wildland fire in the framework of the level set method, Ricerche Mat., 65, 523–533, 2016.

Niemela, J. J. and Sreenivasan, K. R.: Turbulent convection at high Rayleigh numbers and aspect ratio 4, J. Fluid Mech., 557, 411–422, 2006.

Pagnini, G.: A model of wildland fire propagation including random effects by turbulence and fire spotting, in: Proceedings of XXIII Congreso de Ecuaciones Diferenciales y Aplicaciones XIII Congreso de Matemática Aplicada. Castelló, Spain, 9–13 September 2013, pp. 395–403, 2013.

Pagnini, G.: Fire spotting effects in wildland fire propagation, in: Advances in Differential Equations and Applications, edited by Casas, F. and Martínez, V., vol. 4 of *SEMA SIMAI Springer Series*, pp. 203–214, Springer International Publishing Switzerland, dOI 10.1007/978-3-319-06953-1_20. ISBN: 978-3-319-06952-4 (eBook: 978-3-319-06953-1), 2014.

Pagnini, G. and Massidda, L.: Modelling turbulence effects in wildland fire propagation by the randomized level-set method, Tech. Rep. 2012/PM12a, CRS4, Pula (CA), Sardinia, Italy, revised version: August 2014, available at: http://publications.crs4.it/pubdocs/2012/PM12a/pagnini_massidda-levelset.pdf and arXiv:1408.6129, 2012a.

Pagnini, G. and Massidda, L.: The randomized level-set method to model turbulence effects in wildland fire propagation, in: Modelling Fire Behaviour and Risk. Proceedings of the International Conference on Fire Behaviour and Risk. ICFBR 2011, Alghero, Italy, October 4–6 2011, edited by Spano, D., Bacciu, V., Salis, M., and Sirca, C., pp. 126–131, ISBN 978-88-904409-7-7, 2012b.

Pagnini, G. and Mentrelli, A.: Modelling wildland fire propagation by tracking random fronts, Nat. Hazards Earth Syst. Sci., 14, 2249–2263, 2014.

Pagnini, G. and Mentrelli, A.: The randomized level set method and an associated reaction-diffusion equation to model wildland fire propagation, in: Progress in Industrial Mathematics at ECMI 2014, edited by Russo, G., Capasso, V., Nicosia, G., and Romano, V., vol. 22 of *Mathematics in Industry*, pp. 531–540, Springer, Cham, proceedings of The 18th European Conference on Mathematics for Industry, ECMI 2014, Taormina, Italy, June 9–13, 2014, 2016.

Perryman, H. A., Dugaw, C. J., Varner, J. M., and Johnson, D. L.: A cellular automata model to link surface fires to firebrand lift-off and dispersal, Int. J. Wildland Fire, 22, 428–439, 2013.

Porterie, B., Zekri, N., Clerc, J.-P., and Loraud, J.-C.: Modeling forest fire spread and spotting process with small world networks, Combust. Flame, 149, 63–78, 2007.

Pugnet, L., Chong, D., Duff, T., and Tolhurst, K.: Wildland–urban interface (WUI) fire modelling using PHOENIX Rapidfire: A case study in Cavaillon, France, in: MODSIM2013, 20th International Congress on Modelling and Simulation. Modelling and Simulation Society of Australia and New Zealand, December 2013, edited by Piantadosi, J., Anderssen, R., and Boland, J., pp. 228–234, 2013.

Sardoy, N., Consalvi, J. L., Porterie, B., and Fernandez-Pello, A. C.: Modeling transport and combustion of firebrands from burning trees, Combust. Flame, 150, 151–169, 2007.

Sardoy, N., Consalvi, J. L., Kaiss, A., Fernandez-Pello, A. C., and Porterie, B.: Numerical study of ground-level distribution of firebrands generated by line fires, Combust. Flame, 154, 478–488, 2008.

Sofiev, M., Ermakova, T., and Vankevich, R.: Evaluation of the smoke-injection height from wild-land fires using remote-sensing data, Atmos. Chem. Phys., 12, 1995–2006, 2012.

Tarifa, C., del Notario, P., and Moreno, F.: On flight paths and lifetimes of burning particles of wood, in: Tenth Symposium on Combustion', 17–21 August 1964, Cambridge, UK, pp. 1021–1037, The Combustion Institute: Pittsburgh, PA, 1965.

Tarifa, C., del Notario, P., Moreno, F., and Villa, A.: Transport and combustion of firebrands, Technical Report Grants FG-SP-114, FG-SP-146, Instituto Nacional de Tecnica Aeroespacial, 1967.

Thomas, J. C., Mueller, E. V., Santamaria, S., Gallagher, M., El Houssami, M., Filkov, A., Clark, K., Skowronski, N., Hadden, R. M., Mell, W., and Simeoni, A.: Investigation of firebrand generation from an experimental fire: Development of a reliable data collection methodology, Fire Safety J., 91, 864–871, 2017.

Thurston, W., Kepert, J. D., Tory, K. J., and Fawcett, R. J. B.: The contribution of turbulent plume dynamics to long-range spotting, Int. J. Wildland Fire, 26, 317–330, 2017.

Tohidi, A. and Kaye, N. B.: Stochastic modeling of firebrand shower scenarios, Fire Safety J., 91, 91–102, 2017.

Tohidi, A., Kaye, N., and Bridges, W.: Statistical description of firebrand size and shape distribution from coniferous trees for use in Monte Carlo simulations of firebrand flight distance, Fire Safety J., 77, 21–35, 2015.

Tolhurst, K., Shields, B., and Chong, D.: Phoenix: Development and Application of a Bushfire Risk Management Tool, Aust. J. Emerg. Manage., 23, 47–54, 2008.

Tymstra, C., Bryce, R., Wotton, B., Taylor, S., and Armitage, O.: evelopment and structure of Prometheus: the Canadian wild land fire growth simulation model, Information Report NOR-X-417, Canadian Forest Service, Northern Forestry Centre, 2010.

Wadhwani, R., Sutherland, D., Ooi, A., Moinuddin, K., and Thorpe, G.: Verification of a Lagrangian particle model for short-range firebrand transport, Fire Safety J., 91, 776–783, 2017.

Wang, H. H.: Analysis on downwind distribution of firebrands sourced from a wildland fire, Fire Technol., 47, 321–340, 2011.

Woycheese, J. P., Pagni, P., and Liepmann, D.: Brand propagation from large-scale fires, J. Fire Prot. Eng., 10, 32–44, 1999.

Geosci. Model Dev. Discuss., https://doi.org/10.5194/gmd-2018-33
Manuscript under review for journal Geosci. Model Dev.
Discussion started: 19 March 2018

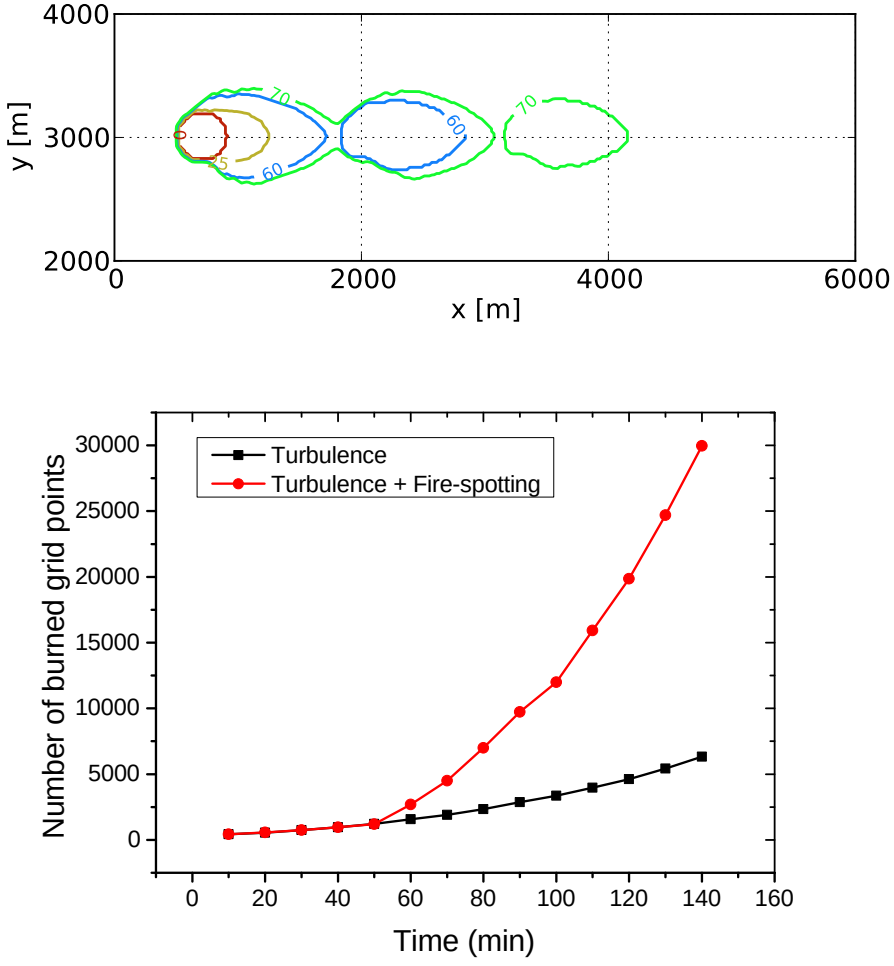

Figure 1. Top panel: Line contours showing the fire perimeter at different time steps. The wind velocity is $10\,\mathrm{ms}^{-1}$, fire intensity is $25\,\mathrm{KWm}^{-1}$ and diffusion coefficient is $0.15\,\mathrm{m}^2\mathrm{s}^{-1}$. The x and y axis of the plot are scaled by a factor of 4. Bottom panel: A comparison of the total burned area at different time steps when only turbulence is considered (black) and when both turbulence and fire-spotting are included (red). The total burned area is simply the number of burned grid points at any each instant. For both line plots, the wind velocity is $10\,\mathrm{ms}^{-1}$, fire intensity is $25\,\mathrm{KWm}^{-1}$ and diffusion coefficient is $0.15\,\mathrm{m}^2\mathrm{s}^{-1}$.

Geosci. Model Dev. Discuss., https://doi.org/10.5194/gmd-2018-33
Manuscript under review for journal Geosci. Model Dev.
Discussion started: 19 March 2018

Geoscientific Model Development Discussions
Open Access
EGU

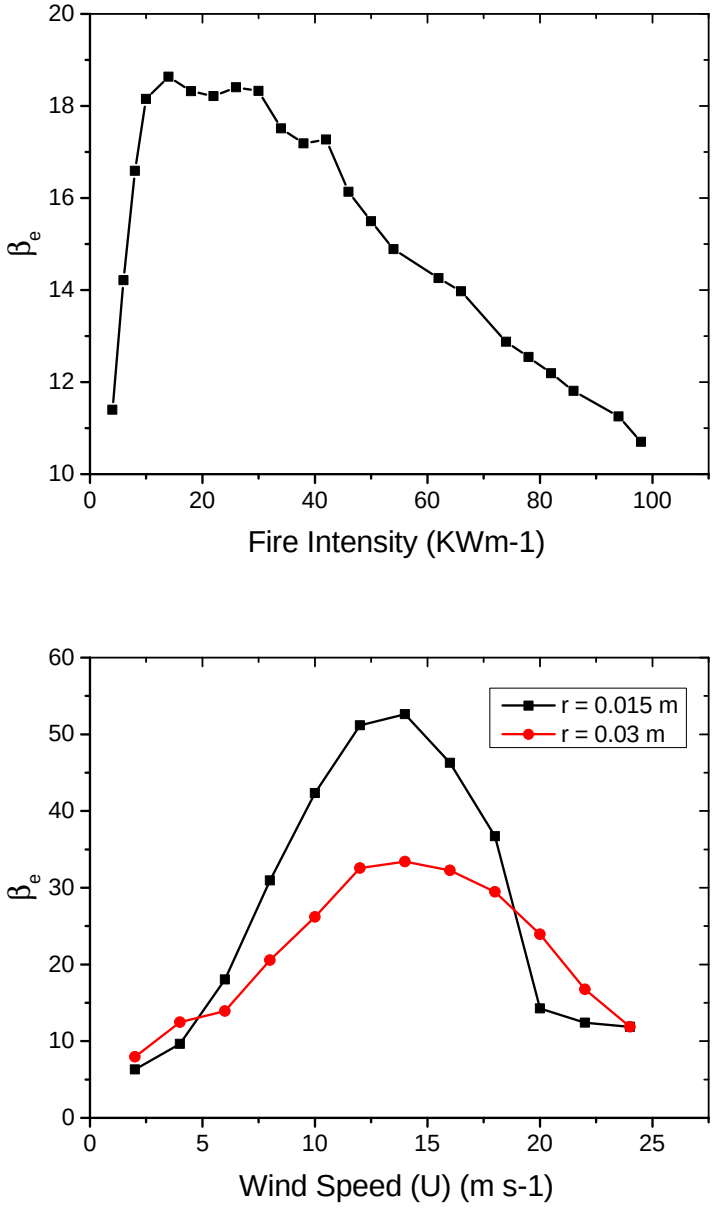

Figure 2. Top panel: Line plot showing the sensitivity of the formulation to different values of fire intensity over constant wind conditions ($10\,\mathrm{ms}^{-1}$) and constant firebrand radius ($0.015\,\mathrm{m}$). The sensitivity is measured in terms of the total increase in the burned area when both fire-spotting and turbulence are included over the case when no random effects are considered. The parameter β_e is defined as : $\beta_e = (\mathbf{x}_{random} - \mathbf{x}_{no-random})/\mathbf{x}_{no-random}$. The diffusion coefficient $\mathcal{D}$ is $0.15\,\mathrm{m}^2\mathrm{s}^{-1}$. Bottom panel: Line plot showing the sensitivity of the formulation to different wind conditions and radii, when fire intensity is constant ($50\,\mathrm{KWm}^{-1}$). The measure of effective increase in area (β_e) and other simulation parameters are the same as defined in the Top panel.